ORIENTAL JOURNAL OF CHEMISTRY
An International Open Free Access, Peer Reviewed Research Journal
www.orientjchem.org
Est. 1984
ISSN: 0970-020 X
CODEN: OJCHEG
2018, Vol. 34, No.(5):
Pg. 2471-2476

New Aromatic Azo-Schiff bases as Carbon Steel Corrosion Inhibitor in 1 M H_2SO_4

HAMIDA EDAN SALMAN[1], ASIM A. BALAKIT[2]* and ALI AHMED ABDULRIDHA[1]

[1]Chemistry Department, College of Education for Pure Sciences, University of Karbala, Iraq.
[2]College of Pharmacy, University of Babylon, Babylon, Iraq.
*Corresponding author E-mail: asim_alsalehi@hotmail.com

http://dx.doi.org/10.13005/ojc/340532

(Received: September 09, 2018; Accepted: September 25, 2018)

ABSTRACT

A new aromatic Schiff base with azo linkage **(AS)** has been synthesized and characterized by FT-IR, ^{1}H NMR and ^{13}C NMR spectroscopic techniques. The new compound **(AS)** has been evaluated as carbon steel corrosion inhibitor at different concentrations (0.005, 0.01, 0.02, 0.04 and 0.08 mM) and different temperatures (303 – 333 K). The corrosion inhibition efficiency was studied by potentiodynamic polarization and weight loss measurements. The effects of concentration and temperature on the inhibition efficiency were studied by potentiodynamic polarization measurements, the results showed that increasing concentration of **AS** increases the inhibition efficiency while increasing the temperature decreases it, the highest corrosion inhibition efficiency, 93.9% was recorded with 0.08 mM of **AS** at 313 K in 1 M H_2SO_4. Weight loss measurements showed that the inhibition efficiency reached 97.1% in the presence of **AS** (0.08 mM) at 313 K. The adsorption process was found to obey Langmuir isotherm, and the adsorption thermodynamic parameters were studied. Scanning electron microscope (SEM) was used to confirm the results.

Keywords: Azo, Schiff base, Carbon steel, Corrosion inhibitors, Organic inhibitors.

INTRODUCTION

Acidic solutions are usually used in industry for variety of purposes such cleaning and descaling of metallic parts; however, such processes are accompanied with the problem of corrosion which is considered as one of the most damaging problems that occur as a result of the dissolution of metals due to the exposure of the metallic parts to the acidic solutions[1-2]. It is well known that carbon steel alloy is the alloy of the choice to be used in the manufacturing of the machines due to its unique mechanical properties. Accordingly, reduction or inhibition of the carbon steel corrosion in acidic environments became an interesting research area. The use of organic materials as corrosion inhibitors is considered as one of the best ways to protect steel alloys form the aggressive acidic attack, they form a shield-like layer after the molecules of the applied inhibitor being adsorbed on the surface of the metal acting as an insulator between the metal and the environment and inhibit the corrosion process[3-5]. It is reported that the presence of π-electrons and heteroatoms such as N, O, P or S in the structure of the aromatic organic molecules makes them effective corrosion inhibitors since they have such

adsorption centers that bind the molecules onto the metal surface forming a protective film[6-11]. Among the reported organic inhibitors ones that contain nitrile (-CN)[12,13], imine (-C=N)[14,15] and/or azo (-N=N-)[16] groups in their structures.

In the present work we report the design, synthesis, and use of new azo-schiff compound as carbon steel corrosion inhibitor in 1.0 M H_2SO_4 solution. The new inhibitor is readily synthesized via two steps synthetic pathway from relatively inexpensive starting materials, it is designed to be rich with π-electrons, has azo (-N=N-), imine (-C=N) and methoxy (-OCH_3) groups in its structure, a non-ionic surfactant tween 80 is used in this study to increase the solubility of the inhibitor and consequently improve the corrosion inhibition efficiency.

EXPERIMENTAL

Preparation of Steel Specimens

Cylindrical carbon steel specimens (24 mm diameter and 3 mm height) composed of: 0.22% C, 0.23% Si, 0.83% Mn, 0.006% P, 0.008% S, 0.79% Cr, 0.33% Mo, 0.08% Ni, 0.02% Al, 0.19% Cu and Fe were used. The specimens were mechanically grounded by grinding and polishing machine with emery papers grade (80 - 3000), a mirror-like surface was obtained after treatment with polishing paste (diamond suspension, 1µm). Finally, samples were rinsed in distilled-water then in absolute ethanol under ultrasonic conditions and kept in a desiccator until used.

Synthesis of the Organic Inhibitor (AS)

The target compound was synthesized via two steps as shown in Scheme 1.

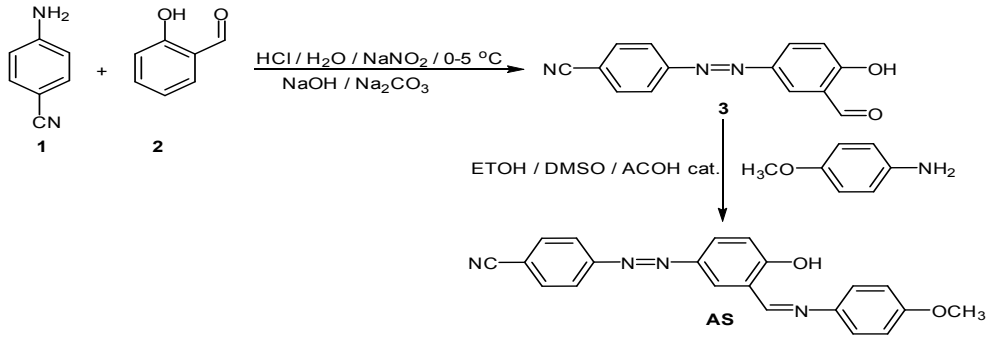

Scheme 1. Synthesis of AS

Compound 3 was synthesized according to a literature procedure[17], then 3 (0.5 gm, 1.99 mmol) was dissolved in DCM (5 ml). 4-Methoxyaniline (0.245 gm, 1.99 mmol) was dissolved in absolute methanol (25 ml), the two solutions were mixed and catalytic amount of glacial acetic acid was added. The reaction mixture was subjected to reflux conditions for 5 hours. The product was collected by filtration and washed with hot methanol. The structure of **AS**, Fig. 1, was characterized by FT-IR, ^{1}H NMR and ^{13}C NMR.

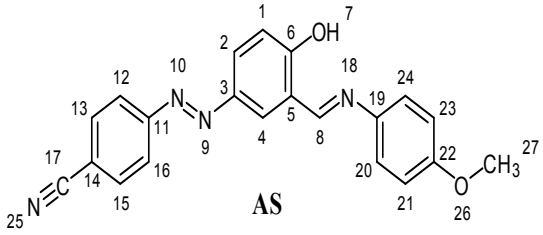

Fig. 1. Structure of AS

Yield 78%. M.P 247-249°C. IR (KBr): 3078(OH), 2227 (C≡N), 1618 (C=N), 1512 (N=N), 1597 (C=C Ar), 2964, 2837 (CH_3).

^{1}H NMR

(400 MHz, DMSO-d_6) δ 14.30 (s, 1H, H-7), 9.13 (s, 1H, H-8), 8.30 (s, 1H, H-4), 8.05 – 7.95 (m, 5H, H-2, 12, 13, 15, 16), 7.5 (d, J = 8.1 Hz, 2 H, H-20, 24), 7.14 (d, J = 8.9, 1H, H-1), 7.10 – 7.01 (d, J = 7.9 Hz, 2H, H-21, 23), 3.82 (s, 3H, H-27).

^{13}C NMR

(101 MHz, DMSO-d_6) δ 165.69(C-6), 160.80(C-8), 159.40 (C-11,12), 134.28(C-3,19), 129.15(C-13,15), 127.73(C-2,4), 123.35 (C-5, 12, 16), 123.23 (C-1, 20, 24), 118.86 (C-17), 115.27 (C-14, 21, 23) , 55.94 (C-27) .

Preparation of Solutions

Different concentrations (0.005, 0.01, 0.02,

0.04 and 0.08 mM) of AS were prepared, 0.029 g of AS was dissolved it in DMSO (2 ml) and 0.01 g of tween 80, then volume was brought up to 1000 ml with of 1.0 M H_2SO_4 to get 0.08 mM concentration which used as stock solution for the preparation of the other concentrations by dilution.

Potentiodynamic Polarization Measurements

Potentiodynamic polarization measurements were carried out by three electrodes cell. Saturated calomel electrode Hg/Hg_2Cl_2 was used as a reference electrode and Pt electrode was used as an auxiliary electrode. The carbon steel specimen was connected to the working electrode with exposure area of 1 cm^2. The working electrode was then dipped in the test solution for (30 min. with a time step of 2 sec). The change in electrode potentials was ±250 mV and sweep rate 0.3 mVs^{-1}. By the extrapolation of Tafel plots segments, the corrosion current density (I_{corr}) was measured. The inhibition efficiency (η%) was calculated according to equation (1)[18].

$$\eta\% = \frac{I_{corr} - I_{inh}}{I_{corr}} x\ 100 \quad (1)$$

Where I_{corr} and I_{inh} represent corrosion current density in the absence and presence of **AS** respectively.

Weight Loss Analysis

Carbon steel specimens were accurately weighed and immersed in the aggressive solution (200 ml, with and without different concentrations of the **AS**) for 3 h at 313 K. Specimens were then washed with distilled water and ethanol under ultrasonic conditions. After drying, specimens were accurately weighed. Duplicate experiments were done in each case. The inhibition efficiency (ηw%) and surface coverage were calculated according to equation (2)and (3) respectively[19,20].

$$\eta w(\%) = \frac{W_o - W}{W_o} x\ 100 \quad (2)$$

$$\eta = \frac{W_o - W}{W_o} \quad (3)$$

Where W and W_o represent the weight loss for the specimen after immersion with and without inhibitors.

Scanning Electron Microscope (SEM) Analysis

The test sample were immersed in the acidic solution (1 M H_2SO_4) for 3 h in the absence and presence of **AS** (0.08 mM) , sample was then washed thoroughly with methanol, dried and tested by SEM.

RESULTS AND DISCUSSION

Potentiodynamic polarization measurements were used to test the corrosion inhibition efficiency of carbon steel by the new compound **AS** in 1 M H_2SO_4. The experiments were carried out at different temperatures (303, 313, 323 and 333 K), in presence of different concentrations of **AS** (0.00, 0.005, 0.01, 0.02, 0.04 and 0.08 mM). Table 1 illustrates the measured parameters that include: corrosion potential (E_{corr}), corrosion current density (I_{corr}), cathodic and anodic Tafel slopes (βc and βa), inhibition efficiency (η%) and surface coverage (θ). The results indicate that increasing the concentration increases the inhibition efficiency at each temperature, the maximum recorded inhibition efficiency was 93.9% in the presence of **AS** in 0.08 mM concentration at 313 K. It was also found that increasing the temperature above 313 K decreases the inhibition efficiency, such decrement in the efficiency may be attributed to the desorption of **AS** molecules form the adsorbed protective film on the metal surface. The displacement in the E_{corr} values that results from the presence of **AS** in the acidic solution was found to be less than 85 mV (Table 1), this indicates that **AS** acts as a mixed type inhibitor which inhibits both anodic and cathodic reactions simultaneously[21]. Fig. 2 shows the obtained polarization curves.

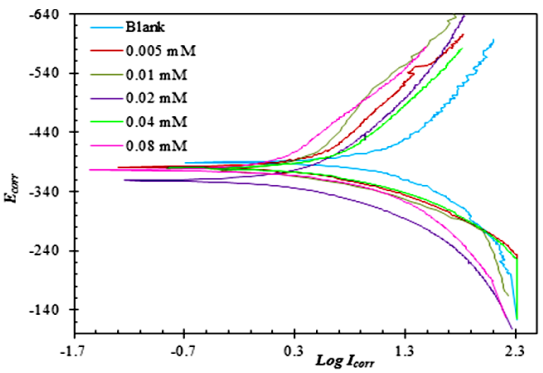

Fig. 2. Potentiodynamic polarization curves for carbon steel in 1 M H_2SO_4 in the absence and presence of AS at 313 K

Table 1: Polarization parameters for carbon steel corrosion in 1 M H_0SO_4 in the presence of different concentrations AS at different temperatures

Temperature (K)	Concentration of AS (mM)	- E_{cor} (mV)	I_{corr} (μA/cm²)	βa (mVdec¹)	- βc (mVdec1)	η%	θ
303		386	7120	60.6	-85.4	0	0
313	0	384.9	7620	88.5	-158.8	0	0
323		384.8	8850	59.6	-86.3	0	0
333		386.6	9110	64.5	-101.8	0	0
303		381.3	2240	43.7	-88.6	68.5	0.68
313	0.005	378.8	1590	34	-77.2	79.1	0.791
323		385.6	4620	48.9	-61.7	47.7	0.477
333		385	6680	50.6	-67.1	26.6	0.266
303		386.1	1520	49.8	-123.6	78.6	0.786
313	0.01	373.9	1240	32	-79.9	83.7	0.837
323		381	3880	76	-151.5	56.1	0.561
333		379.5	5500	36.5	-41.6	39.6	0.396
303		380	1310	35.6	-61.8	81.6	0.816
313	0.02	359.1	1010	40.2	-56.5	86.7	0.867
323		383.2	3390	33.5	-54.1	61.6	0.616
333		380.5	4830	57	-85.5	46.9	0.469
303		380.8	856.16	24.5	-37.6	87.9	0.879
313	0.04	379	824.37	18.5	-22.3	89.1	0.891
323		385.6	2370	32.9	-44.1	73.2	0.732
333		374.6	3860	63.9	-107.2	57.6	0.576
303		379.6	611.19	21.3	-34.9	91.4	0.914
313	0.08	375.7	464.83	15.8	-38.1	93.9	0.939
323		384.5	1450	28.4	-36.7	83.6	0.836
333		384.8	2340	58.6	-125.5	74.3	0.743

Weight Loss Measurements

Weight loss measurements were performed using different concentrations of **AS** at 313 K (the optimum temperature determined from the potentiodynamic polarization measurements); Table 2 shows the obtained results. It was found that the corrosion inhibition efficiency increases as the inhibitor's concentration increases, this could be attributed to the increment of the adsorbed molecules of **AS** on the metal surface (higher surface coverage) forming most effective protecting film, the maximum inhibition efficiency (97.1%) was observed at the highest concentration of **AS** (0.08 mM).

Table 2: Inhibition efficiencies of AS according to weight loss measurements

AS Concentration (mM)	Inhibition efficiency ηw%	Surface coverage η
0.005	89.8	0.898
0.01	92.9	0.929
0.02	93.1	0.931
0.04	93.3	0.933
0.08	97.1	0.971

Adsorption Isotherm

A linear plot was obtained from plotting C_{inh}/θ versus C_{inh}, indicating that the adsorption of **AS** on the metal surface obeys Langmuir isotherm, Fig. 3 shows Langmuir isotherms of **AS** at 303 – 33 K. Equations (3) and (4) were used to calculate the equilibrium constant (K_{ads}) and Gibbs' free energy (ΔG_{ads}) of the adsorption process[22, 23].

$$C_{inh}/\theta = = \frac{1}{K_{ads}} + C_{inh} \quad (3)$$

$$\Delta G_{ads} = -RT \ln(55.5\ K_{ads}.) \quad (4)$$

Where C_{inh} is concentration of the **AS**, θ is the surface coverage, *T* is the temperature and *R* is the universal gas constant. The numerical value of 55.5 represents the molar concentration of water in the acid solution. To determine the values of standard enthalpy change (ΔH_{ads}), log K_{ads} was plotted versus 1/T (Fig. 4) and the ΔH_{ads} values were calculated according Van't Hoff equation(5)[24].

$$\log K_{ads} = \left(-\frac{\Delta H_{ads}}{2.303\ R\ T}\right) + \text{Constant} \quad (5)$$

The standard entropy change (ΔH_{ads}) values were calculated according to equation(6)[25].

$$\Delta G_{ads} = \Delta H_{ads} - T\Delta S_{ads} \quad (6)$$

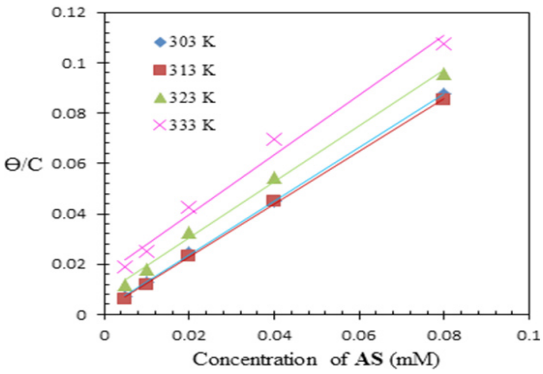

Fig. 3. Langmuir adsorption isotherms of AS at different temperatures 303 – 33 K.

The calculated thermodynamic parameters for the adsorption process are shown in Table 3. The high values of K_{ads} indicate that there is a high affinity for **AS** to be adsorbed on the metal surface forming the protective film and leading to the high inhibition efficiency. From the negative values of ΔG

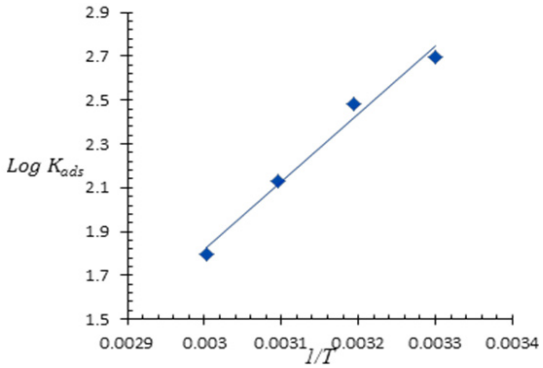

Fig. 4. log K_{ads} versus 1/T for AS

denote that the adsorption process is spontaneous, and confirms the stability of the adsorbed film on the carbon steel surface; furthermore, its value indicates the physisorption process[26].

SEM Analysis

To confirm the high corrosion inhibition efficiency of **AS**, SEM was used to study the effect of the aggressive acidic solution on the surface of the carbon steel in the presence and absence of **AS** by visualizing the damage caused as a result of the corrosion process, Fig. 5 shows the obtained images with 10 µm scale. It is clear that the surface of the uninhibited sample (absence of **AS**, Fig. 4 A) is severely damaged due to the acid corrosion, while the surface of the inhibited sample (presence of **AS**, Fig. 4 B) is smoother and no significant damage was observed, this confirms that AS is acting as excellent corrosion inhibitor.

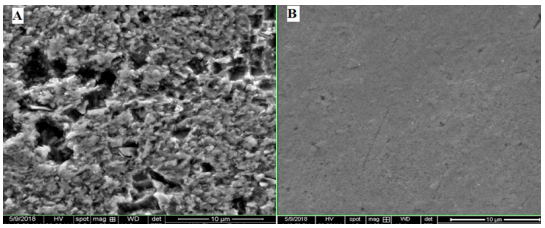

Fig. 5. SEM images of uninhibited (A) and inhibited (B) carbon steel surface

Table 3: The calculated thermodynamic parameters for the adsorption of AS

Temperature (K)	K_{ads} (M^{-1})	ΔG_{ads} (kJ mol^{-1})	ΔS_{ads} (kJ mol^{-1})	ΔH_{ads} (kJ mol^{-1})
303	500	-25.77	-0.10933	-58.9
313	303.0303	-25.32	-0.10728	
323	135.1351	-23.96	-0.10817	
333	62.5	-22.56	-0.109129	

CONCLUSION

A new azo-schiff compound (**AS**) has been synthesized, the inhibition efficiency of AS for carbon steel corrosion in 1 M H_2SO_4 was investigated, tween 80 was used as a surfactant to improve the solubility

of the inhibitor. High inhibition efficiency was recorded (93.3% by potentiodynamic polarization and 97.1% by weight loss measurements) at 0.08 mM concentration. Thermodynamic studies proved that **AS** is spontaneously adsorbed on the carbon steel surface via physisorption interaction forming a stable protecting film in the aggressive acidic environment. Such high corrosion inhibition efficiency with such low concertation make **AS** an excellent carbon steel corrosion inhibitor with environmental and economic advantages.

ACKNOWLEDGMENT

The authors thank the University of Karbala and the University of Babylon for the financial support.

REFERENCES

1. Verma, C., Olasunkanmi, L. O., Ebenso, E. E., Quraishi, M.A., *Results in physics*., **2018**, *8*, 657-670.
2. Douadi, T., Hamani, H., Daoud, D., Al-Noaimi, M. and Chafaa, S., *Journal of the Taiwan Institute of Chemical Engineers*., **2017**, *71*, 388-404.
3. Douadi, T., Hamani, H., Daoud, D., Al-Noaimi, M., Chafaa, S., *Journal of the Taiwan Institute of Chemical Engineers*., **2017**, *71*, 388-404.
4. Dutta, A., Saha, S.K., Adhikari, U., Banerjee, P., Sukul, D., *Corrosion Science*., **2017**, *123*, 256-266.
5. Finšgar, M., Jackson, *J., Corrosion Science*., **2014**, *86*, 17-41.
6. Amin, M. A., Mohsen, Q., Hazzazi, O.A., *Materials Chemistry and Physics*., **2009**, *114*(2-3), 908-914.
7. Verma, C., Quraishi, M.A., Olasunkanmi, L.O., Ebenso, E.E., *RSC Advances*., **2015**, *5*(104), 85417-85430.
8. Danaee, I., Niknejad Khomami, M., *Material wissenschaft und Werkstofftechnik*., **2012**, *43*(11), 942-949.
9. Ghasemi, O., Danaee, I., Rashed, G.R., RashvandAvei, M., Maddahy, M.H., *Journal of Central South University*., **2013**, *20*(2), 301-311.
10. El Haleem, S.A., El Wanees, S.A., El Aal, E.A., Farouk, A., *Corrosion Science*., **2013**, *68*, 1-13.
11. Lai, C., Xie, B., Zou, L., Zheng, X., Ma, X., Zhu, S., *Results in physics*., **2014**, *7*, 3434-3443.
12. Fouda, A.S., Rashwan, S.M., Farag, M.E., *Protection of Metals and Physical Chemistry of Surfaces*., **2015**, *51*(4), 637-650.
13. Fouda, A.S., Diab, M.A., Fathy, S., *International Journal of Electrochemical Science*., **2017**, *12*(1), 347-362.
14. Benabid, S., Douadi, T., Issaadi, S., Penverne, C., Chafaa, S., *Measurement*., **2017**, *99*, 53-63Q
15. Hosseini, M., Mertens, S.F., Ghorbani, M., Arshadi, M.R., *Materials Chemistry and Physics*., **2003**, *78*(3), 800-808.
16. Bedair, M.A., El-Sabbah, M.M.B., Fouda, A.S., Elaryian, H.M., *Corrosion Science*., **2017**, *128*, 54-72
17. Bouchouit, M., Elkouari, Y., Messaadia, L., Bouraiou, A., Arroudj, S., Bouacida, S., Taboukhat, S., Bouchouit, K., *Optical and Quantum Electronics*., **2016**, *48*(3), 178.
18. Singh, D. K., Ebenso, E. E., Singh, M. K., BEHERA, D., Udayabhanu, G., John, R. P., *Journal of Molecular Liquids*., **2018**, *250*, 88-99.
19. Golestani, G., Shahidi, M., Ghazanfari, D., *Applied Surface Science*., **2014**, *308*, 347-362.
20. Ansari, K.R., Quraishi, M.A. and Singh, A., *Measurement*., **2015**, *76*, 136-147.
21. Tezcan, F., Yerlikaya, G., Mahmood, A. and Kardas, G., *Journal of Molecular Liquids*., **2018**, *269*, 398-406.
22. Verma, C., Ebenso, E., Bahadur, I., Obot, I., Quraishi, M., *Journal of Molecular Liquids.,* **2015**, *212*, 209-218.
23. Verma, C., Quraishi, M., Singh, A., *Journal of Molecular Liquids*., **2015**, *212*, 804-812.
24. Fouda, A.S., Hassan, A.F., Elmorsi, M.A., Fayed, T.A. and Abdelhakim, A., *Int. J. Electrochem. Sci*., **2014**, *9*, 1298-1320.
25. Chaouiki, A., Lgaz, H., Chung, I.M., Ali, I.H., Gaonkar, S.L., Bhat, K.S., Salghi, R., Oudda, H. and Khan, M.I., *Journal of Molecular Liquids*., **2018**, *266*, 603-616.
26. Hassan, M., *Materials Letters*., **2018**, *15*, 82-84.